Strong Motion Simulation for the Philippines Based on Seismic Hazard Assessment

Ribelito F. Torregosa*

*Graduate student, Department of Civil Engineering, Gifu University, Japan

Masata Sugito**

**Professor, Department of Civil Engineering, Gifu University, Japan

Nobuoto Nojima***

***Assoc. Professor, Department of Civil Engineering, Gifu University, Japan

ABSTRACT

A simulation technique for strong ground motion based on seismic hazard analysis for the Philippines that incorporates both historical earthquakes and active faults is presented. The database for historical earthquake occurrences from 1907 to 1998, provided by the Philippine Institute of Volcanology and Seismology (PHIVOLCS) was used. Philippine active faults identified from various geotectonic studies of the country were compiled. Seismic source zoning for the Philippines was based on the occurrence rates of historical earthquakes. A polygonal source area model was used to represent seismic source zones. Estimation formulas for peak ground acceleration (A_{max}) and effective ground acceleration (A_e), used with the JMA scale of seismic intensity, were developed from 118 components of selected strong ground motion records for engineering foundation levels in Japan. Expected ground motion parameters corresponding to both rare events of 475 years recurrence (10% in 50 years) and occasional events of 100 years recurrence (39% in 50 years) in the Philippines were determined. Hazard-consistent magnitudes and hypo-central distances from different source zones for the three major Philippine cities, Manila, Cebu, and Davao, were obtained probabilistically, and their respective acceleration, velocity, and displacement time histories simulated.

1. INTRODUCTION

The Philippines is located in one of the most seismically active regions of Asia. Many destructive earthquakes have occurred in various parts of the country. One of the most notable was the 1990 Central Luzon earthquake with a magnitude of MS=7. 6. The Philippine trench, formed by subduction of the western edge of the Philippine plate under the Eurasia plate, is one of the country's major seismic generators. Other major seismic generators are the Philippine fault and Manila trench, which roughly parallel the Philippine trench. These three major faults have high slip rates of more than 6. 5 cm per year. Many other faults have been traced in the country, but details are unavailable because many are located on the sea bottom.

Past seismic hazard studies for the Philippines, based on historical earthquakes, were made by Acharya et al. (1979), Villaraza (1991) and Molas and Yamazaki (1994). Acharya (1980a) used active fault data to study the seismic hazard in the Philippines, but no published report has incorporated both historical earthquakes and active faults. Through the seismic monitoring agency (PHIVOLCS), the Philippine government is now reviewing active Philippine faults. Currently there are about 34 seismological stations distributed throughout the islands of the Philippines. Most of them were installed in the 1990s after the destructive 1990 Central Luzon earthquake. Up to now, no major ground motion records

have been obtained.

Past probabilistic seismic hazard studies for the Philippines were concerned only with maximum ground motion intensity, such as peak ground acceleration (A_{max}). Peak ground acceleration (A_{max}) for different levels of exceedance probabilities for all areas of the country have been studied. Although the seismic hazard for the country is high, other ground motion parameters, such as peak ground velocity (V_{max}) and the response spectra for different levels of exceedance probabilities have not been studied. A method for generating strong ground motions by means of seismic hazard analysis is presented. Scenario earthquakes were simulated for the country's major cities because of their vulnerability to earthquake damage.

Major parts of this study are: a) a probabilistic seismic hazard analysis of the Philippines based on both historical earthquakes and active faults, b) determination of expected peak ground motion parameters for earthquake events with 475 and 100 years recurrences, and c) simulation of ground motion time histories for the three major cities of the Philippines based on seismic hazards.

2. EARTHQUAKE DATA IN THE PHILIPPINES

2.1 Historical earthquake occurrence data

This information was obtained from the Philippine Institute of Volcanology and Seismology (PHIVOLCS). Data for 5969 histor-
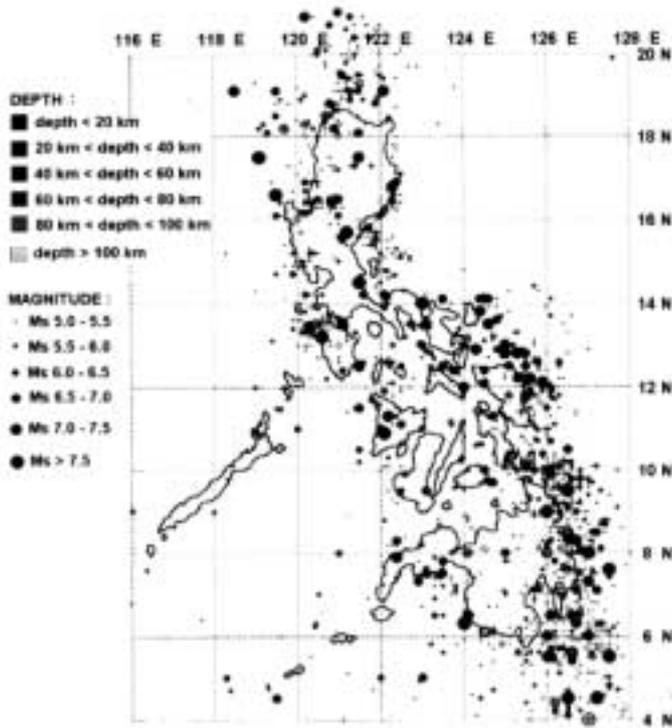
Fig. 1   Sites of historical earthquakes (1907-1998)

a) Magnitude range (4.0 - 4.4)

b) Magnitude range (4.5 - 5.9)
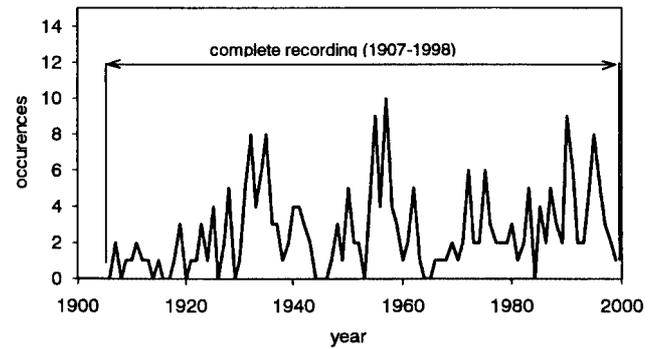
c) Magnitude range > 5.9

Fig. 2   Yearly occurrences of earthquakes by magnitude

ical earthquakes (Lanuza, 1999) recorded since 1907 were used. Locations of main shocks with surface wave magnitudes of $M_s \geq 5.0$ are shown in Fig. 1.

Because the collected earthquake records are incomplete for $M_s < 6.0$, the years of complete records for different magnitude ranges had to be determined. The yearly occurrences of earthquakes for $M_s \geq 4.0$ were analyzed. The incompleteness of historical earthquake information can be grouped into the three magnitude ranges. These are; $M_s \geq 6.0$, $4.5 \leq M_s \leq 5.9$, and $4.0 \leq M_s \leq 4.4$. The yearly occurrences of earthquakes for these three magnitude ranges are plotted in Fig. 2, from which the period in which complete records of historical earthquakes in the Philippines are assumed to be:

1) $M_s \geq 6.0$ records are complete from *1907 – 1998*
2) $4.5 \leq M_s \leq 5.9$ records are complete from *1962 – 1998*
3) $4.0 \leq M_s \leq 4.4$ records are complete from *1975 – 1998*

The period with complete records of lower magnitude earthquakes is too short. In order to maximize the use of all the historical earthquake occurrences, corrections were made to quantities of each magnitude since 1907 for which there are no complete records. These corrections (Katayama, 1982) were added to the quantity of each data taking into consideration the incompleteness of the records.

Assuming that the occurrence of an earthquake with the given magnitude, i, is random and independent of past events, the occurrence rate, v_i, is:

$$v_i = \frac{n_i}{t_i} \qquad (1)$$

Where n_i is the number of earthquakes of magnitude i, and t_i is the period of complete observation. The average occurrence rate, v, from magnitude, j to k, is written:

$$v = \sum_{i=j}^{k} v_i = \sum_{i=j}^{k} \frac{n_i}{t_i} \qquad (2)$$

Letting T be the reference period,

$$v = \frac{1}{T} \cdot \sum_{i=j}^{k} \left(n_i \cdot \frac{T}{t_i} \right) \qquad (3)$$

$\frac{T}{t_i}$ is the correction factor for different magnitude ranges taking into consideration the reference time period, T, and the time of complete recording, t_i. Here, the reference time period T, is 92 years (from 1907 - 1998). The correction factors are computed as follows:

1) For $M_s \geq 6.0$; $\frac{T}{t_i} = \frac{92}{92} = 1.0$

2) For $4.5 \leq M_s \leq 5.9$; $\frac{T}{t_i} = \frac{92}{37} = 2.48$

3) For $M_s \le 4.4$; $\dfrac{T}{t_i} = \dfrac{92}{92} = 1.0$

The total numbers of occurrences within the above specified magnitude ranges were multiplied by the correction factors.

2.2   Seismic source zones

A significant factor in seismic hazard analysis is the division of seismic source zones, in which seismic activity can be treated as homogenous. Rast and Saegesser (1980) showed the effects of varying the seismic source zones. They pointed out that variation in seismic source zoning accounts for as much as half the difference in the results and that the other half is due to different assumptions, such as the upper bounds on magnitude and other factors. Seismic source zoning therefore must be done systematically, the seismic characteristics of each individual source zone consequently being homogenous. To ensure that the designated seismic source zones used in the hazard analysis had homogenous seismic characteristics, the occurrence rates of earthquakes for the entire country were calculated. The spatial moving average method was used to determine the occurrence rates of earthquakes at individual points in the country. In that procedure, the occurrence rate at a point is determined by dividing the number of occurrences within a 100km radius by the area of a circle with a 100km radius to obtain the average number of occurrences per square kilometer at the point. The result is then divided by the number of years covered by our data to obtain the occurrences per

Table 1.   Seismic source zone properties

Zone	Occurrence rate per sq. km.	b value	Max. Magnitude (Ms)	Area sq. km.
1	1.46E-05	0.940	7.3	46,222
2	1.49E-05	1.056	7.2	56,146
3	6.60E-05	1.571	6.9	30,350
4	2.94E-05	1.458	6.5	15,471
5	6.40E-05	1.431	6.6	15,218
6	1.33E-05	1.093	7.7	49,207
7	4.17E-05	1.215	7.8	16,097
8	5.96E-05	1.792	7.0	36,812
9	1.35E-04	1.489	7.7	12,770
10	6.37E-06	0.598	7.6	52,699
11	2.04E-05	1.217	7.1	40,324
12	1.23E-05	0.743	7.4	50,285
13	1.96E-05	1.043	8.3	51,934
14	8.10E-05	1.072	7.3	28,801
15	1.51E-05	1.939	6.0	23,956
16	1.38E-04	1.453	7.7	25,913
17	1.41E-05	1.353	6.3	28,149
18	6.28E-06	1.330	6.7	75,851
19	3.50E-05	1.210	7.0	43,450
20	1.17E-05	0.888	7.3	40,179
21	3.36E-05	1.074	7.9	20,630
22	1.26E-05	1.130	7.3	60,709
23	3.46E-05	1.429	7.4	38,975
24	1.04E-04	1.274	7.7	28,658
25	1.23E-04	1.301	7.3	28,074
26	3.24E-05	0.880	7.9	29,076
27	3.33E-06	1.111	6.5	89,574
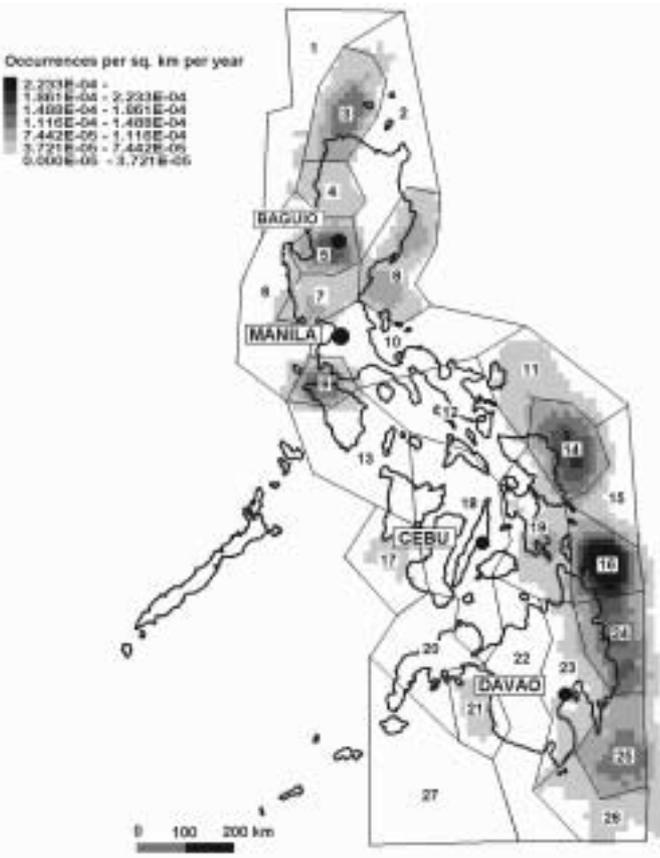
Fig. 3   Seismic source zones
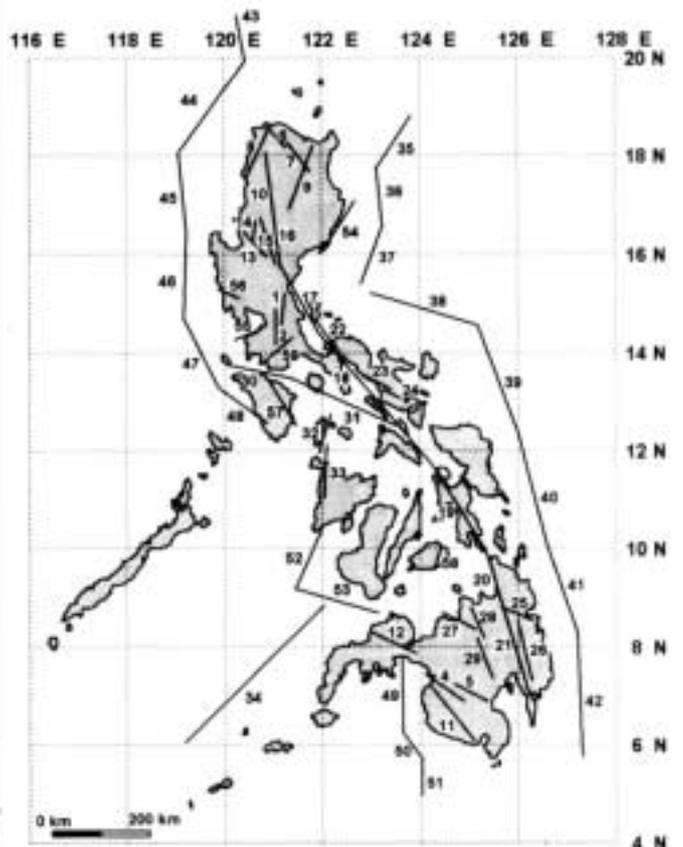
Fig. 4   Philippine active faults (Acharya, 1980a; Knittel, et al, 1988; Barrier, et al, 1991; Sajona, et al, 1993)

square kilometer per year. In this paper, the number of occurrences per square kilometer per year per point is called the occurrence rate. Occurrence rates of all the points in the Philippines for $M_s \geq 4.0$ were calculated using the above procedure. Polygons were drawn enclosing adjacent areas with nearly uniform occurrence rates. Each polygon was designated a single seismic source zone, for which uniform random occurrences of earthquakes are assumed. Totally, 27 source zones were designated by this method. These source zones and the occurrence rates are shown in Fig. 3. Linear regression analysis was done to obtain the **b**-value of each seismic source zone. The properties of each zone (occurrence rate, **b**-value, maximum magnitudes, and area) are given in Table 1. No seismic source zone was assigned to the western portion of the Philippines which historically has had very few, widely scattered earthquakes.

2.3 Active fault data

Fifty-nine active faults were compiled from the previous reports of Acharya (1980a), Knittel (1988), Barrier, et al. (1991), and Sajona et al. (1993), (Fig. 4). Their fault parameters are given in Table 2.

To incorporate the effect of active faults in the seismic hazard evaluation, the parameters of maximum credible earthquake (MCE) and recurrence MCE time are indispensable. Slemmons (1978) determined the percent of fault rupture to total fault length during a maximum earthquake for strike-slip faults longer than 280 kilometers. Because the active faults in the Philippines are of the strike-slip type, his fault-rupture relation was used. Slemmons' relationship between total fault length, L, and percentage rupture, λ, during maximum earthquake is

$$\lambda = 15.76 + 0.012 \cdot L \qquad (4)$$

where:

λ = percentage of rupture (i.e., $\dfrac{\text{ruptured length}}{\text{total fault length}} \times 100\%$)

L = fault length in km

Table 2. Philippine active fault parameters

Segment number	Fault	Length (km)	Rupture length (km)	Max expected magnitude	Occurrence rate per year
1	Marikina fault segment 1	70	35.2	6.3	1.82E-03
2	Marikina fault segment 2	80	40.1	6.4	1.43E-03
3	Marikina fault segment 3	80	40.1	6.4	1.43E-03
4	Cotabato fault segment 1	87	43.3	6.4	1.43E-03
5	Cotabato fault segment 2	108	54.0	6.6	1.11E-03
6	Abra1	144	71.8	6.8	8.33E-04
7	Abra2	144	71.8	6.8	8.33E-04
8	Abra3	128	64.0	6.7	1.00E-03
9	Abra4	152	75.9	6.9	5.56E-04
10	Abra5	144	71.9	6.8	8.33E-04
11	Mindanao1	168	84.1	6.9	5.56E-04
12	Mindanao2	116	57.8	6.7	1.00E-03
13	Phil. FaultLuzon 1	77	38.5	6.3	1.82E-03
14	Phil. Fault Luzon 2	50	25.0	6.0	2.50E-03
15	Phil. Fault Luzon 3	113	56.4	6.6	1.11E-03
16	Phil. Fault Luzon 4	119	59.7	6.7	1.00E-03
17 - 21	Phil. Fault	1127	330.0	8.0	5.00E-03
22	Phil. Fault Bicol segment 1	122	60.9	6.7	1.00E-03
23	Phil. Fault Bicol segment 2	70	35.1	6.3	1.82E-03
24	Phil. Fault Bicol segment 3	51	25.7	6.0	2.50E-03
25	Phil. Fault Surigao segment	75	37.6	6.3	1.82E-03
26	Phil. Fault Davao segment	143	71.5	6.8	8.33E-04
27	Cental Mindanao Fault segment 1	92	46.1	6.5	1.25E-03
28	Cental Mindanao Fault segment 2	73	36.3	6.3	1.82E-03
29	Cental Mindanao Fault segment 3	95	47.6	6.5	1.25E-03
30	Lubang/Verde Passage Fault	152	75.8	6.9	5.56E-04
31	Sibuyan Sea Fault	240	120.2	7.2	5.00E-04
32	Tablas Fault1	107	53.7	6.6	1.11E-03
33	Tablas Fault2	121	60.5	6.7	1.00E-03
34	Sulu Trench	535	118.7	7.2	6.67E-04
35 - 38	East Luzon trench	530	117.2	7.2	6.67E-03
39 - 42	Philippine Trench	1258	388.2	8.1	6.67E-03
43 - 48	Manila Trench	1042	294.5	7.9	5.00E-03
49 - 51	Cotabato Trench	320	62.7	6.7	1.00E-03
52 - 53	Negros Trench	336	66.5	6.8	8.33E-04
54	Casigura Fault	134	66.8	6.8	8.33E-04
55	Manila Bay Fracture Zone	59	29.6	6.1	2.50E-04
56	Iba Fracture ZoneAcharya	50	25.0	6.0	2.86E-04
57	Mindoro faullt	114	56.8	6.6	1.11E-03
58	Bohol fault	52	25.8	6.0	2.50E-03
59	Taal Fracture Zone	85	42.7	6.4	1.43E-04

This relationship was used for faults longer than 280 kilometers. Rupture lengths during maximum events for faults with lengths of 50 to 280 kilometers are assumed to be half the total length as in Mualchin (1996). All the active faults included in this study are more than 50 kilometers long. Other possible scenarios of fault ruptures, such as smaller events with higher annual occurrence frequencies, are neglected. Acharya (1980b) studied the relationship between magnitude and fault rupture in Philippine earthquakes. That relationship is

$$M_S = 1.79 \cdot \text{Log}_{10} R_F + 3.5 \tag{5}$$

where:

R_F = fault rupture length (λL) in kilometers

M_S = magnitude (*surface wave*)

The maximum credible earthquake magnitude of each active Philippine fault was determined by substituting the rupture length in Eq. (5). The recurrence times of expected maximum magnitudes were determined by Slemmons (1978) method.

3. PROBABILISTIC SEISMIC HAZARD ANALYSIS

3.1 A brief overview of the theory (Kameda and Nojima, 1988)

Seismic hazard analysis deals with probabilistic models of earthquake occurrences. Identifying the exact location of future earthquakes is very difficult at this stage. In dealing with seismic hazards, it is acceptable to assume that earthquakes occur randomly both in size and location within a source zone. This assumption is modeled by the Poisson process. In the Poisson model, the only parameter is the mean rate of earthquake occurrence. For seismic hazards from fault sources, the Poisson model can be used with the maximum credible earthquake magnitude determined deterministically from the fault length and the expected recurrence period.

The annual probability that the random earthquake intensity, Γ, at a specific site will exceed the value, γ, assuming the Poisson process, is

$$p_0 = 1 - \exp\left\{-\sum_{k=1}^{n} v_k q_k(\gamma)\right\} \cong \sum_{k=1}^{n} v_k q_k(\gamma) \tag{6}$$

in which n is the number of potential earthquake sources in the region of a site, v_k the earthquake occurrence rate in source k with upper and lower boundary magnitudes of m_{uk} and m_{lk}, and $q_k(\gamma)$ the probability that the random earthquake intensity, G, will exceed the given intensity, γ, given that an earthquake occurs in source k.

$$q_k(\gamma) = \int_{m_{lk}}^{m_{uk}} \int_{r_{lk}}^{r_{uk}} P(\Gamma > \gamma | m, r) f_{MK}(m) f_{RK}(r) \, dmdr \tag{7}$$

in which $f_{Mk}(r)$ is the probability density function of magnitude m in source k, $f_{Rk}(r)$ the probability density function of distance r (upper and lower value= r_{uk}, r_{lk}) in source k, and P($\Gamma > \gamma | m, r$) the probability of ($\Gamma > \gamma$) for a given m and r. When uncertainty in the attenuation formula of peak ground motion is involved, the attenuation rule $\Gamma = \gamma_E(m,r)$ is given by $\Gamma = U \cdot \gamma_E(m,r)$, in which U is the lognormal variate representing attenuation uncertainty with a median of 1.0 and coefficient of variation δ_γ. This gives

$$P(\Gamma > \gamma | m,r) = P(U \cdot \gamma_E(m, r) > \gamma)$$
$$= P\left(U > \frac{\gamma}{\gamma_E(m, r)}\right) \tag{8}$$

The hazard curve is obtained by calculating p_0 from Eq. (6) for various values of δ_γ, allowing determination of the value $\gamma_0(p_0)$ of the intensity parameter corresponding to a specified p_0.

Let x represent any ground motion parameter being discussed. Assume that it is represented as a function of earthquake magnitude, m, and distance r.

$$x = \phi(m,r) \tag{9}$$

The conditional mean of x for source k, given that $\Gamma > \gamma_0(p_0)$ is

$$\bar{x}_k(p_0) = E\left[x | \Gamma > \gamma_0(p_0) \cap E_k\right]$$
$$= \int_M \int_R \phi(m,r) f_{M,R|\Gamma > \gamma_0(p_0)}(m,r) drdm$$
$$= \frac{1}{q_k(\gamma_0)} \int_M \int_R \phi(m,r) P\left(U > \frac{\gamma_0(p_0)}{\gamma_E(m,r)}\right) f_{MK}(m) f_{RK}(r) drdm \tag{10}$$

in which E_k represents the earthquake that occurs in source k, and $f_{M,R}|\Gamma > \gamma_0(p_0)(m,r)$ the conditional joint probability density function of the magnitude and distance, given that $\Gamma > \gamma_0(p_0)$. When all potential earthquake sources are considered, the conditional mean of x is

$$\bar{x}(p_0) = \frac{\sum_{k=1}^{n} \bar{x}_k(p_0) v_k q_k(\gamma_0)}{\sum_{k=1}^{n} v_k q_k(\gamma_0)}$$

$$\bar{x}(p_0) = \frac{\sum_{k=1}^{n} v_k \int_M \int_R \phi(m,r) P\left(U > \frac{\gamma_0(p_0)}{\gamma_E(m,r)}\right) f_{Mk}(m) f_{Rk}(r) drdm}{\sum_{k=1}^{n} v_k \int_M \int_R P\left(U > \frac{\gamma_0(p_0)}{\gamma_E(m,r)}\right) f_{Mk}(m) f_{Rk}(r) drdm} \tag{11}$$

The conditional mean of the magnitude, $\bar{m}_k(p_0)$, and that of the distance from the seismic source zone k, $\bar{r}_k(p_0)$, respectively are given by Eqs. (12) and (13), and are referred to as the hazard-consistent magnitude and distance (Kameda and Nojima, 1988):

$$\bar{m}(p_0) = \frac{\int_M \int_R m \cdot P\left(U > \frac{\gamma_0(p_0)}{\gamma_E(m,r)}\right) f_{MK}(m) f_{Rk}(r) drdm}{\int_M \int_R P\left(U > \frac{\gamma_0(p_0)}{\gamma_E(m,r)}\right) f_{MK}(m) f_{Rk}(r) drdm} \tag{12}$$

$$\bar{r}_k(p_0) = \frac{\int_M \int_R r \cdot P\left(U > \frac{\gamma_0(p_0)}{\gamma_E(m,r)}\right) f_{Mk}(m) f_{Rk}(r) drdm}{\int_M \int_R P\left(U > \frac{\gamma_0(p_0)}{\gamma_E(m,r)}\right) f_{Mk}(m) f_{Rk}(r) drdm} \tag{13}$$

3.2 Seismic hazards from fault sources

The expected maximum earthquake magnitude and shortest distance from the site to the fault were assumed to be the parameters that would cause the fault to produce a seismic hazard. The expected maximum earthquake magnitude from active fault M_k^F, obtained deterministically, is discussed in section 2.3. To obtain the seismic hazard caused by a fault, the $q_k(\gamma)$ given in Eq. 7 is modified to:

$$q_k^F(\gamma) = P(\Gamma > \gamma | M_k^F, R_k^F) \tag{14}$$

in which M_k^F is the expected maximum magnitude for fault k, and R_k^F the shortest distance from fault k to the site:

$$P(\Gamma>\gamma|M_k^F,R_k^F)=P\left(U>\frac{\gamma}{\gamma_E(M_k^F,R_k^F)}\right) \qquad (15)$$

Let x represent the ground motion parameter due to the maximum earthquake magnitude from fault k. It is a function of M_k^F and R_k^F;

$$x_k^F=\psi(M_k^F,R_k^F) \qquad (16)$$

The ground motion parameter, x_k^F, for fault k, given that $\Gamma>\gamma_0(p_0)$ is

$$x_k^F(p_0)=E\left[x_k^F\,\middle|\,\Gamma>\gamma_0(p0)\cap E_K\right]$$
$$=\frac{1}{q_k^F(\gamma_0)}\psi(M_k^F,R_k^F)P\left(U>\frac{\gamma_0(p_0)}{\gamma_E(M_k^F,R_k^F)}\right) \qquad (17)$$

When all potential fault sources are considered, the conditional mean of x_k^F is

$$\bar{x}^F(p_0)=\frac{\sum\limits_{k=1}^{n^F}x_k^F(p_0)\cdot v_k^F\cdot q_k^F(\gamma_0)}{\sum\limits_{k=1}^{n^F}v_k^F\cdot q_k^F(\gamma_0)}$$
$$=\frac{\sum\limits_{k=1}^{n^F}\psi(M_k^F,R_k^F)\cdot v_k^F\cdot P\left(U>\frac{\gamma_0(p_0)}{\gamma_E(M_k^F,R_k^F)}\right)}{\sum\limits_{k=1}^{n^F}v_k^F\cdot P\left(U>\frac{\gamma_0(p_0)}{\gamma_E(M_k^F,R_k^F)}\right)} \qquad (18)$$

in which v_k^F is the occurrence rate per year of M_k^F. Combining the effects of both the historical earthquakes and n^F number of active faults, the conditional mean of $x(p_0)$ is

$$\bar{x}(p_0)=\frac{\sum\limits_{k=1}^{n}v_k\int_M\int_R\phi(m,r)P(\Gamma>\gamma_0(p_0))f_{Mk}(m)f_{Rk}(r)drdm+}{\sum\limits_{k=1}^{n}v_k\int_M\int_RP(\Gamma>\gamma_0(p_0))f_{Mk}(m)f_{Rk}(r)drdm+}$$
$$\frac{\sum\limits_{k=1}^{n^F}v_k^F\psi(M_k^F,R_k^F)\cdot P(\Gamma>\gamma_0(p_0))}{\sum\limits_{k=1}^{n^F}v_k^F\cdot P(\Gamma>\gamma_0(p_0))} \qquad (19)$$

Seismic hazards corresponding to a moderate annual exceedance probability (p_0), are dominated by the contribution from historical earthquakes, whereas those for a very low annual exceedance probability is dominated by the contribution from fault sources. The historical earthquake data used coveres earthquakes from 1907 to 1998. Historical earthquakes associated with the rupture of active faults, other than the 1990 Central Luzon earthquake, are not included. Maximum credible earthquake magnitudes from active faults show a minimum recurrence interval of several hundred years. Historical events covered by the data are assumed not to be associated with this known active faults.

3.3 Attenuation formula for rock surface ground motions

Sugito et al. (2000) developed a database of modified strong motion records for engineering foundation levels with shear wave velocities of 500-600 m/sec using the major Japanese strong motion records. These records obtained on deposit sites were converted to the equivalent free rock level surface motion by the modified equivalent linearization method for the response analysis of layered ground, the FDEL, developed by Sugito (1995). Fig. 5 shows the scattergrams of the database for 118 components of rock surface ground motion time histories that was used for regression analysis in order to develop the attenuation formula for rock surface ground motion.

Based on this database, linear regression analysis was performed to formulate the attenuation formula for peak ground acceleration (A_{max}) and effective ground acceleration (A_e). Herein, the ground motion parameter, A_e, used in the JMA Seismic Intensity scale, I_{JMA}, is dealt with. Parameter A_e, called 'effective acceleration', is obtained from filtered acceleration time histories. The JMA seismic intensity I_{JMA} is scaled in

$$I_{JMA}=2\cdot\log_{10}A_e+0.94 \qquad (20)$$
where:
I_{JMA} = seismic intensity (JMA scale)
A_e = effective peak acceleration

According to the definition of A_e by the JMA, its effective acceleration is determined from the vector synthesis of three orthogonal components of ground acceleration time histories obtained from the three components of the filtered acceleration time histories. Here only A_e determined from a single component of the time history is dealt with, because the dataset for rock surface ground motion does not include vertical component time histories.
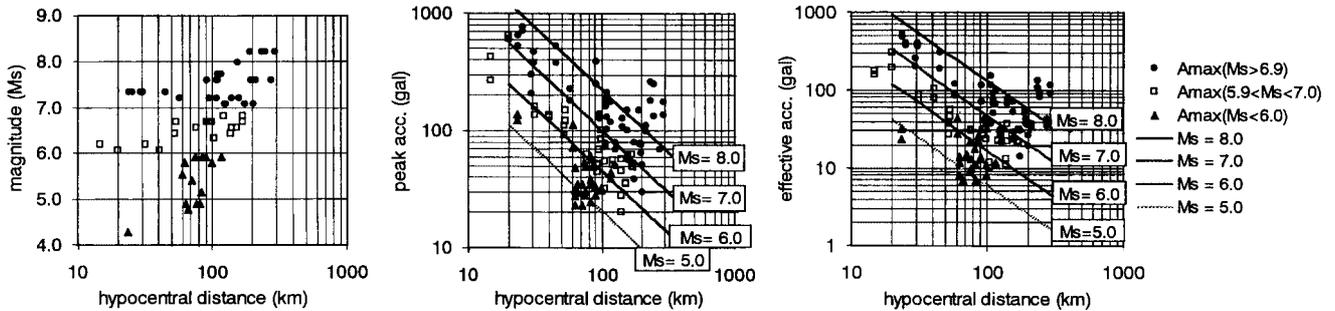
a) magnitude and distance   b) peak acceleration and hypo-central distance   c) effective acceleration and hypo-central distance

Fig. 5   Scattergrams of the modified rock-surface strong motion dataset

The database is in JMA magnitude scale, M_J, therefore the empirical formula for converting M_J to M_S, proposed by Hayashi and Abe (1984) and given in Eq. (21) is used.

$$M_S = 1.27 \cdot M_J - 1.83 \qquad (21)$$

Linear regression analysis was performed on the dataset given in Table 3 to formulate the attenuation formula for rock surface

Table 3. Datasets of modified rock-surface strong motion records from Japanese earthquakes

No.	year-mo/day-time	M_J	Station	Hyp. Dist.	Comp.	A_{max} (gal)	A_e (gal)
1	1968-0401-0000	7.5	ITAJIMABASHI	110.5	LG	102.2	51
2					TR	129.6	67
3			HOSOSHIMA-S	117.0	N-S	118.4	67
4					E-W	174.9	98
5	1968-0516-0000	7.9	MURORAN-S	293.7	N-S	174.3	114
6					E-W	134.7	89
7			AOMORI-S	247.8	N-S	246.8	94
8					E-W	133.0	82
9			MIYAKO-S	190.1	N-S	149.8	53
10					E-W	149.4	50
11			HACHINOHE-S	235.8	N-S	258.5	107
12					E-W	178.2	130
13	1968-0516-0001	7.4	MURORAN-S	197.0	N-S	75.1	39
14					E-W	63.9	36
15			AOMORI-S	194.0	N-S	75.1	37
16					E-W	77.8	42
17			MIYAKO-S	213.9	N-S	110.0	37
18					E-W	98.3	33
19	1969-0421-0000	6.5	HOSOSHIMA-S	53.0	N-S	90.4	27
20					E-W	110.2	37
21	1970-0726-0000	6.7	HOSOSHIMA-S	54.1	N-S	120.5	46
22					E-W	147.3	56
23	1978-0612-0000	7.4	SHIOGAMA-KOJO-S	107.7	N-S	184.2	116
24					E-W	159.9	152
25			OFUNATO-BOHCHI-S	110.5	N41E	180.1	77
26					E41S	210.4	91
27			HACHINOHE-S	275.9	N-S	68.3	42
28					E-W	69.6	35
29			KAIHOKUBASHI	91.9	LG	250.1	71
30					TR	382.9	114
31	1978-0220-0000	6.7	KAIHOKUBASHI	99.3	LG	84.8	24
32					TR	100.9	32
33	1982-0321-0000	7.1	MURORAN-S	142.7	N-S	107.5	76
34					E-W	126.1	66
35	1982-0723-0000	7.0	ONAHAMA-JI-S	127.6	E-W	49.9	21
36					N-S	49.9	26
37	1983-0526-0000	7.7	AOMORI-S	156.6	E-W	149.1	71
38					N-S	99.9	52
39	1983-0621-0000	7.1	AOMORI-S	160.1	E-W	62.8	29
40					N-S	56.3	23
41	1983-0826-0523	6.8	HOSOSHIMA-S	170.0	E-W	62.8	22
42					N-S	49.3	21
43			OITA-S	121.6	E-W	55.6	22
44					N-S	51.5	23
45	1984-0807-0406	7.1	HOSOSHIMA-S	57.6	E-W	224.3	117
46					N-S	179.2	84
47			OITA-S	108.2	E-W	76.9	40
48					N-S	72.6	37
49	1986-0624-1153	6.5	YAMASHITA-HEN-M	139.3	N-S	27.8	13
50					E-W	20.1	11
51	1987-0114-2003	7.0	KUSHIRO-JI-S	175.2	E-W	78.5	30
52					N-S	39.0	14
53			MURORAN-S	202.0	E-W	50.9	26
54					N-S	29.9	19
55	1987-0206-2216	6.7	SHIOGAMA-KOJO-S	171.3	E-W	51.9	31
56					N-S	48.2	21
57	1987-0318-1236	6.6	OITA-S	152.7	E-W	34.9	24
58					N-S	36.0	26
59			MIYAZAKI-M	77.0	N-S	62.4	30
60					E-W	56.3	31

ground motion. The resulting relationships for rock surface peak ground acceleration (A_{max}) and the effective ground acceleration (A_e) attenuation with the coefficients of variation are given in Table 4. The dataset used to formulate rock level ground motion attenuation relationships has the minimum hypo-central distance of 20 kilometers. Fig. 5 shows the attenuation curves for magnitudes M_S=8.0, 7.0, 6.0, and 5.0.

Table 3.   Datasets of modified rock-surface strong motion records from Japanese earthquakes (continued)

No.	year-mo/day-time	M_J	Station	Hyp. Dist.	Comp.	A_{max} (gal)	A_e (gal)
61	1987-0407-0940	6.6	SHIOGAMA-KOJO-S	140.9	E-W	57.7	37
62					N-S	45.2	22
63			SHINAGAWA-S	93.0	E-W	44.5	27
64	1987-1217-1108	6.7			N-S	51.2	31
65			YAMASHITA-HEN-M	95.7	N-S	69.7	31
66					E-W	52.0	26
67	1989-1102-0325	7.1	MIYAKO-S	96.7	E-W	125.6	43
68					N-S	138.3	39
69	1987-0114-2003	7.0	TOKACHI-M	126.2	N-S	68.1	31
70					E-W	79.1	26
71	1988-0507-1059	6.4	TOKACHI-M	104.9	N-S	32.0	10
72					E-W	54.6	12
73			PORTISLAND	25.4	N-S	700.3	400
74					E-W	750.1	364
75			KEPCO-SOKEN	45.3	N-S	376.2	183
76					E-W	522.7	303
77	1995-0117-0546	7.2	KEPCO-TAKASAGO	29.7	N-S	206.1	198
78					E-W	299.8	254
79			KEPCO-SHINKOBE	30.6	N-S	378.0	352
80					E-W	459.8	391
81			JMA-KOBE-MET	23.8	N-S	644.8	519
82					E-W	521.1	469
83			KG005-MIYANOJO	14.8	N-S	266.2	172
84	1997-0326-1731	6.3			E-W	426.5	157
85			KG006-YOKOGAWA	31.7	N-S	135.9	88
86					E-W	158.0	74
87			KG005-MIYANOJO	20.1	N-S	649.7	191
88	1997-0513-1438	6.2			E-W	603.2	305
89			KG006-YOKOGAWA	40.5	N-S	129.0	103
90					E-W	135.3	79
91	1968-0701-0000	6.1	SHINAGAWA-S	85.8	N-S	50.8	26
92					E-W	49.8	23
93	1966-0820-0000	4.8	SUSOHANADAM	23.3	N-S	122.9	24
94					E-W	137.5	32
95	1982-0306-0000	5.3	HOSOSHIMA-S	76.2	E-W	30.8	10
96					N-S	49.6	13
97	1982-0307-0000	5.5	ONAHAMA-JI-S	82.8	E-W	34.8	11
98					N-S	24.7	7
99			OFUNATO-BOHCHI-S	74.6	S15W	28.4	9
100	1982-0601-0000	6.1			W15N	53.4	22
101			MIYAKO-S	117.0	E-W	39.3	11
102					N-S	44.7	12
103	1982-0812-0000	5.7	YAMASHITA-6-S	70.7	E33S	22.9	14
104					S33W	35.1	15
105	1982-0816-0000	5.3	ONAHAMA-JI-S	63.3	E-W	28.0	12
106					N-S	23.1	8
107	1982-0522-0000	5.2	TOKACHI-M	66.2	N-S	29.7	7
108					E-W	35.4	7
109	1983-0702-0704	5.8	ONAHAMA-JI-S	60.5	E-W	113.5	44
110					N-S	71.5	28
111	1983-0808-1248	6.0	YAMASHITA-HEN-S	63.0	E-W	31.2	14
112					N-S	49.2	14
113	1985-1004-2126	6.1	SHINAGAWA-S	90.2	E-W	33.2	14
114					N-S	28.3	13
115	1988-0318-0534	6.0	YAMASHITA-HEN-M	99.0	N-S	32.7	8
116					E-W	31.2	11
117	1988-0812-1415	5.3	YAMASHITA-HEN-M	81.9	N-S	61.0	18
118					E-W	38.2	11

3.4 Seismic hazard analysis of the Philippines

A seismic hazard analysis that incorporated the effects of both active faults and historical earthquakes was made for the entire land area of the country. Totally, 123,727 points were analyzed; equivalent to a grid size of 1.4 kilometers. The historical earthquake information included only those data for focal depths of less than 100 kilometers. The average focal depth of historical earthquakes with magnitudes greater than M_s=5.0 is 25.4 kilometers. When historical earthquakes are categorized as land and sea events, the respective average focal depths become 21.7 and 27.0 km. Most of the deeper events were located under the sea far from the main islands. Assuming a uniform depth equal to the average value of the total underestimates the hazard because most inland events have focal depths that are less than the average for all the data. In the analysis, a conservative assumption of a 20 kilometer focal depth was used to calculate the seismic hazards. The expected earthquake peak ground motion parameters for occasional (100-year recurrence period) and rare (475- year recurrence period) events for all the land areas of the country were calculated. Figs. 6 and 7, respectively show the expected peak ground accelerations for the 100- and 475-year recurrence periods.

The strong motion records in Japan, used to formulate the attenuation relationships, are earthquake intensity records based on the JMA scale. The attenuation relationship for effective ground accelerations, given in Eq. 23 was used. As ground accelerations are related to earthquake intensities, Eq. 20 was used to convert the effective ground accelerations to the equivalent JMA seismic intensity. The expected seismic intensities on the JMA scale for the 100- and 475-year recurrence periods are shown in Figs. 8 and 9. A graphical correlation of the JMA and MMI intensity scales is shown in Fig. 10.

Locations of the three major Philippine cities: Manila, Cebu, and Davao are shown in Fig. 3. Islands shown without color on the map (an indication of seismic hazard) belong to aseismic areas where no analysis was done. Results show that the eastern Philippines has the highest seismic hazard. These sites are located in zones with a high occurrence rate due to movement of the Philippine plate whose western edge runs along the eastern side of the Philippines. Zones 14 and 16 mainly contributed to the maximum seismic hazard in and around the areas. The expected peak

Table 4. Attenuation formula for rock surface ground motion

Attenuation formula		Coef. of variation
$\log A_{max} = 0.346 \cdot M - 1.056 \cdot \log \cdot R + 1.6945$	(22)	0.444
$\log A_e = 0.446 \cdot M - 1.205 \cdot Log \cdot R + 0.964$	(23)	0.433

R = hypo-central distance in kilometers, M = earthquake magnitude (M_S)
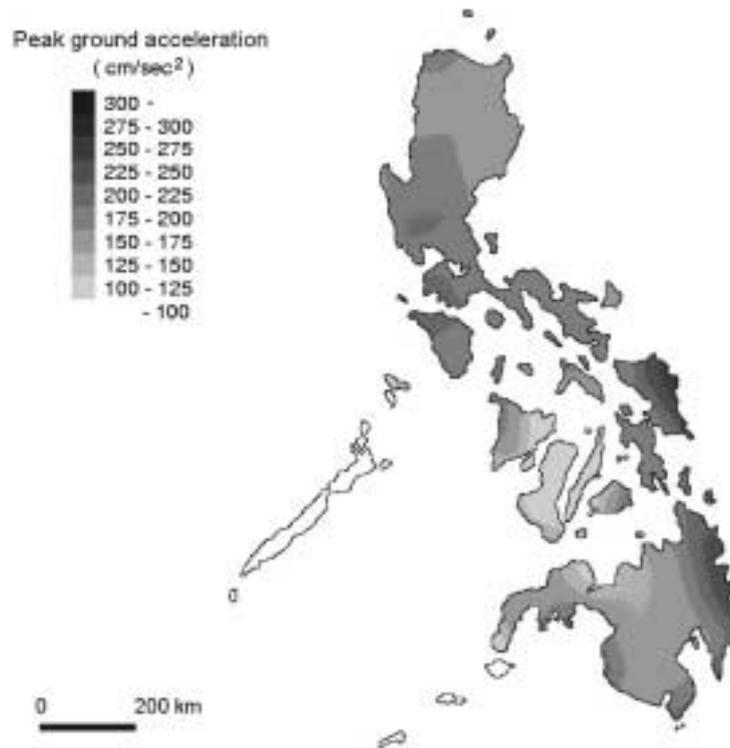
Fig. 6 100-year-recurrence peak ground acceleration map (historical earthquakes and active faults)
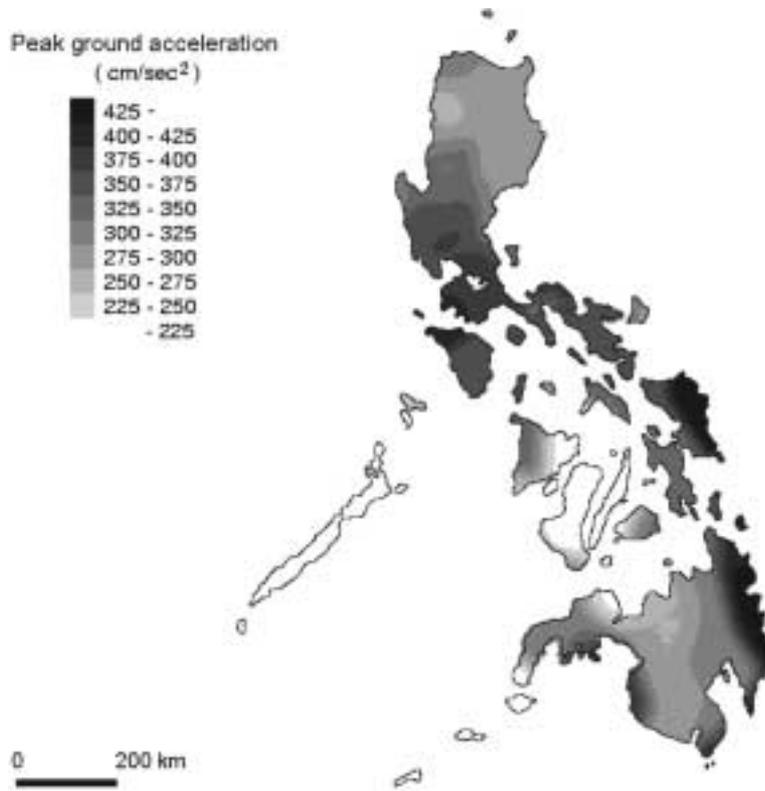
Fig. 7   475-year-recurrence peak ground acceleration map (historical earthquakes and active faults)
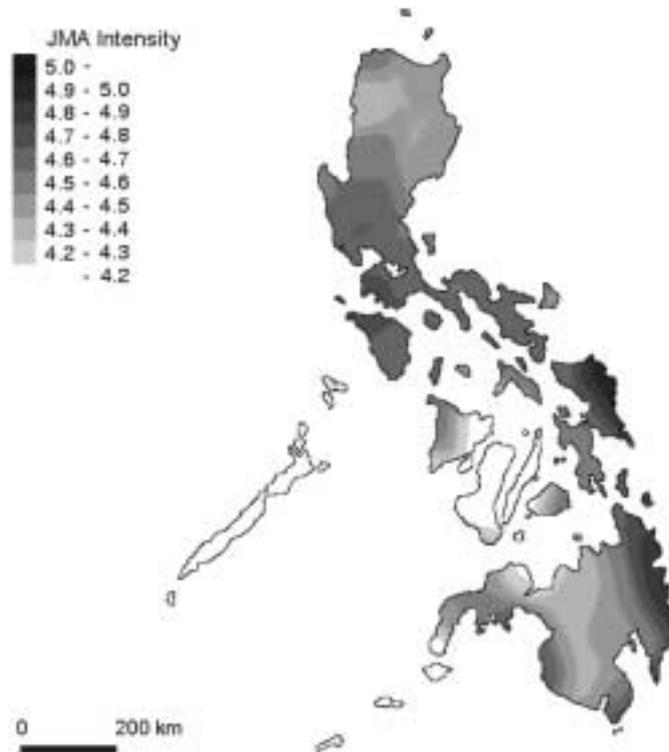
Fig. 8   100-year-recurrence JMA Seismic Intensity map (historical earthquakes and active faults)

ground acceleration for the 100-year recurrence period has a maximum value of 257 gal and that for the 475-year recurrence period 468 gal. The expected seismic intensities on the JMA scale for the 100- and 475-year recurrence periods respectively have the maximum values of 4.9 (VIII in MMI) and 5.5 (IX in MMI). All the maximum values are located inside zone 14. No analysis was made of the western most side of the Philippines where there have been few and scattered historical earthquakes.

The 100-year recurrence peak ground acceleration map compiled for this study is compared with the results of Molas and Yamazaki (1994). In both studies, relatively high seismic hazards are present for eastern Mindanao Island. There are slight differences in the results for the seismic hazards of Luzon. From Molas and Yamazaki's 100-year recurrence peak ground acceleration map, areas surrounding Baguio City, which experienced a destructive earthquake in 1990, have an A_{max} of 200 gal or more, whereas other Central Luzon areas and the Metro Manila area have an A_{max} of less than 100 gal. Clusters of high peak ground accelerations of as much as 600 gal also were found in their study. In our study, a uniform 100-year recurrence peak ground acceleration ranging from 180 – 199 gal is expected in Baguio City, Central Luzon island, and Metro Manila. The maximum inland 100-year peak ground acceleration is only 250 gal. One factor contributing to the differences in the results of the two studies is the different source zones used. The analysis done by Molas and Yamazaki (1994), the seismic hazard was calculated by treating a circular area with a
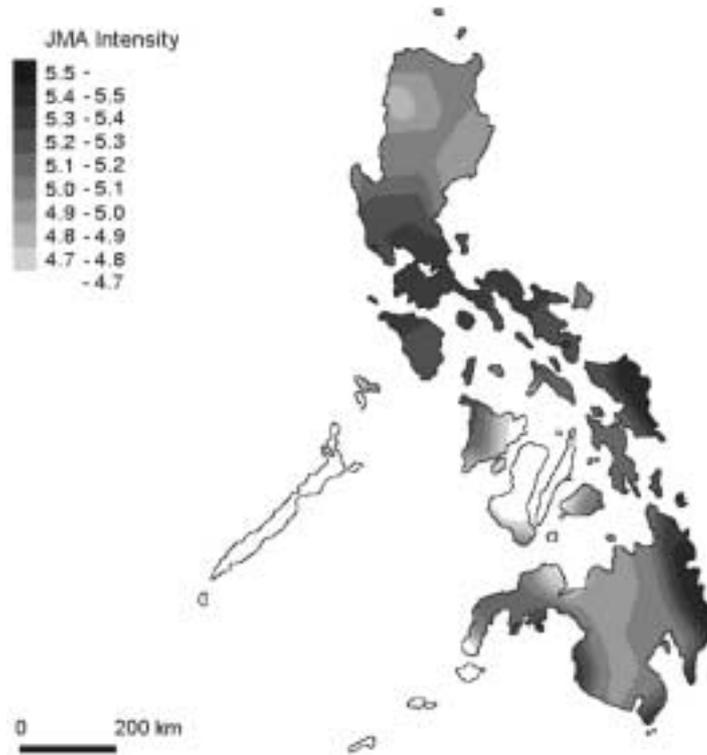
Fig. 9   475-year-recurrence JMA Seismic Intensity map (historical earthquakes and active faults)

Fig. 10   Graphical correlation between the Modified Mercalli (MMI) and JMA intensity scales (ATC-13, 1985)
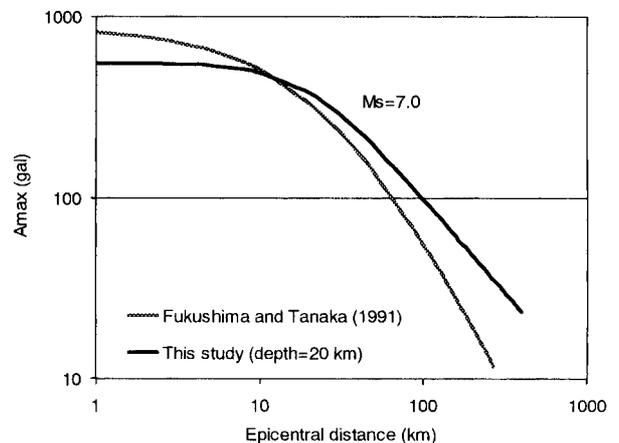
Fig. 11   Comparison of peak ground acceleration attenuation with distance

radius of 250 km around the site as the seismogenic zone. In our analysis, the seismogenic source zones were fixed prior to making the hazard analysis. Another factor is the difference in the attenuation relationships used in the studies. The attenuation formula for peak ground acceleration that they used was reported by Fukushima and Tanaka (1991). A comparison of the peak ground acceleration attenuation relationships used in our and Molas and Yamazaki's studies is shown in Fig. 11.

4. HAZARD-CONSISTENT STRONG MOTION TIME HISTORIES FOR THE MAJOR PHILIPPINE CITIES

4.1 Strong motion prediction on a rock surface

Sugito, et al. (2000) developed a strong motion prediction model based on 118 components of a modified rock surface strong motion dataset obtained from Japanese accelerograms (Table 3). Their simulation model was developed for motion on stiff ground with a shear wave velocity of v_s=500~600 m/sec. This stiff ground is called a "free rock surface". In their model, by use of a given magnitude and hypo-central distance, strong motion time history can be simulated. In that strong motion prediction model, the earthquake acceleration with non-stationary frequency content is

$$x(t) = \sum_{k=1}^{m} \sqrt{4\pi \cdot G_x(t, 2\pi f_k) \Delta f} \cdot \cos(2\pi f_k t + \phi_k) \qquad (24)$$

in which $\sqrt{G_x(t, 2\pi f_k)}$ is the evolutionary power spectrum (Kameda, 1975) for time t and frequency f_k, ϕ_k the independent random phase angles distributed over 0~2π, and m the number of superposed harmonic components. The upper and lower boundary frequencies, f_u and f_l, are fixed as f_u = 10.03 Hz and f_l = 0.13 Hz, and m and Δf are fixed as m = 166 and Δf = 0.06 Hz. The following time-varying function is adopted for the model of $\sqrt{G_x(t, 2\pi f_k)}$;

$$\sqrt{G_x(t, 2\pi f)} = \alpha_m(f) \frac{t - t_s(f)}{t_p(f)} \exp(1 - \frac{t - t_s(f)}{t_p(f)}) \quad ; t > t_s(f) \qquad (25)$$

in which t_s and t_p respectively are the starting time and duration parameter, and $\alpha_m(f)$ is the intensity parameter which represents the peak value of $\sqrt{G_x(t, 2\pi f_k)}$. For each individual frequency, these parameters have been scaled as a function of the magnitude, M,

and hypo-central distance, R. Estimation formulas for the parameters which were modeled as a function of earthquake magnitude and hypo-central distance, as well as for the frequency f, are given in Table 5. Ground motion time history with non-stationary frequency contents can be simulated for a given earthquake magnitude and hypo-central distance. Simulated rock surface ground motions for two combinations of magnitude and hypo-central distance are shown in Fig. 12. The ground motion duration clearly is longer for case (a), and is a typical characteristic of ground motion time history.

4.2 Strong motion simulation based on hazard-consistent earthquake parameters

Seismic hazard analysis was performed for the three biggest cities in the Philippines: Manila, Cebu and Davao. Figure 13 shows the peak ground acceleration, A_{max}, hazard curves for these cities. The hazard curves were determined by combining the contributions of the various seismogenic source zones and active faults. Clearly, Cebu has the least A_{max} hazard. The peak ground acceleration hazard curves for Manila and Davao indicate that A_{max} <144 gal has a higher annual occurrence probability in Davao, whereas A_{max}>144 gal has a higher probability in Manila. This is attributed to the differences in the properties of the seismogenic

Table 5.   Estimation formula for strong motion prediction model parameters (Sugito, 2000)

$\log \alpha_m(f) = B_0(f) + B_1(f) \cdot M - B_2(f) \cdot \log(R)$	(26)
$B_0(f) = -0.657 + 1.637 \cdot \log f - 1.642 \cdot (\log f)^2$ $B_1(f) = 0.563 - 0.208 \cdot \log f + 0.0198 \cdot (\log f)^2$ $B_2(f) = 1.335 - 0.115 \cdot \log f - 0.443 \cdot (\log f)^2$	(27)
$\log t_p(f) = P_0(f) + P_1(f) \cdot M - P_2(f) \cdot \log(R)$	(28)
$P_0(f) = -0.808 - 0.929 \cdot \log f$ $P_1(f) = 0.123 + 0.134 \cdot \log f$ $P_2(f) = 0.357 - 0.083 \cdot \log f$	(29)
$\hat{t}_s(f) = t_s(f) - t_m = S_0(f) + S_1(f) \cdot R$	(30)
$S_0(f) = 0.0 \,(\text{fixed})$ $S_1(f) = \left(0.863 - 0.509 \cdot \log f - 1.141(\log f)^2\right) \times 10^{-2}$	(31)

a) MAGNITUDE = 7.5 HYPOCENTRAL DISTANCE = 100.0 km

b) MAGNITUDE = 6.5 HYPOCENTRAL DISTANCE = 30.0 km
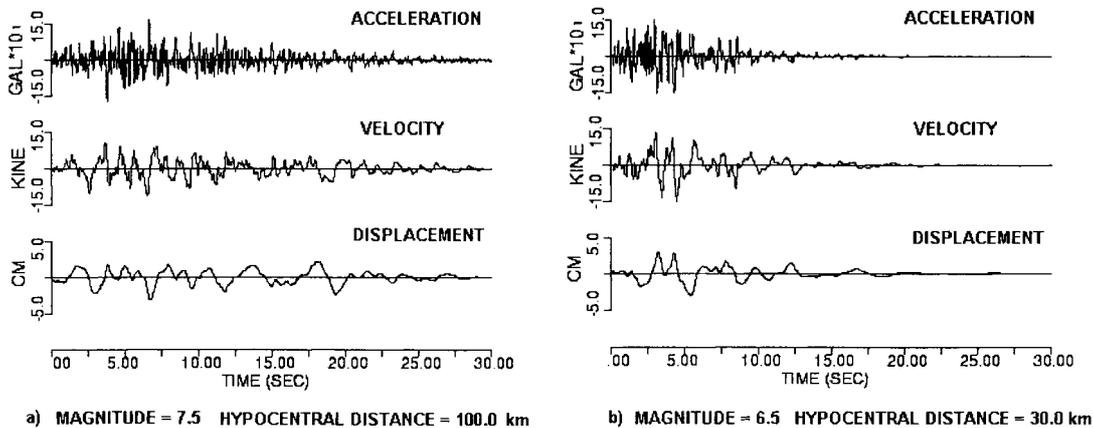
Fig. 12   Simulated rock surface ground motions for two combinations of magnitude and hypo-central distance

zone locations of the two cities. Zone 10, in which Manila is located, has both a lower occurrence rate and b-value than zone 23, in which Davao is located, indicative that Davao has more earthquakes due to its higher occurrence rate. The maximum earthquake magnitude in zone 10 (M_s=7.7), however, is higher than in zone 23 (M_s=7.4). Moreover, the b-value for zone 10 is much lower than that for zone 23; therefore, high magnitude earthquakes are more likely to occur in the Manila area than in Davao. The high A_{max} has a higher annual occurrence probability in Manila than in Davao, whereas the opposite is true for the low A_{max}. Seismic hazard contributions from various source zones were determined, and the seismic hazards from source zone locations shown to dominate the contributions of the three cities, contributions from outside source zones in all cases being negligible (Fig. 14). Because of this, it was decided to determine the hazard-consistent magnitude and hypo-central distances of these three cities based only on their respective zone locations. Manila, Cebu, and Davao respectively are located inside zones 10, 18, and 25. Their hazard-consistent magnitudes and hazard-consistent hypo-central distances are shown in Fig. 15. From Figs. 14 and 15, hazard-consistent magnitudes and the hypo-central distances of these three major
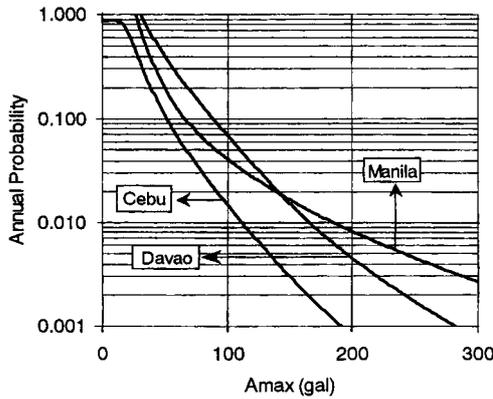
Fig. 13 Peak ground acceleration hazard curves for Manila, Cebu, and Davao

Table 6. Hazard-consistent earthquake parameters

	T = 100 years			T = 475 years		
	Magnitude		Hypo-central	Magnitude		Hypo-central
	M_S	M_J	Distance (km)	M_S	M_J	Distance (km)
Manila	6.8	6.8	40.1	7.1	7.0	32.2
Cebu	5.7	5.9	32.0	5.9	6.1	28.8
Davao	6.0	6.2	30.3	6.5	6.5	28.9
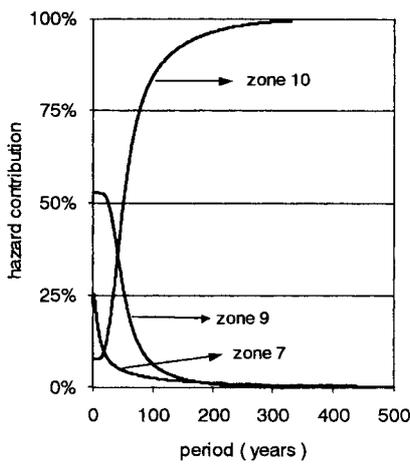
a) Hazard contributions for Manila b) Hazard contributions for Cebu c) Hazard contributions for Davao
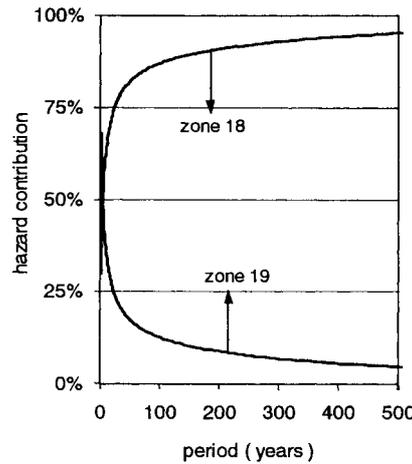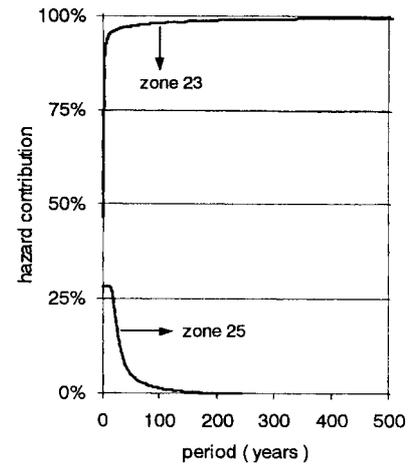
Fig. 14 Hazard contribution curves for the three major Philippines cities
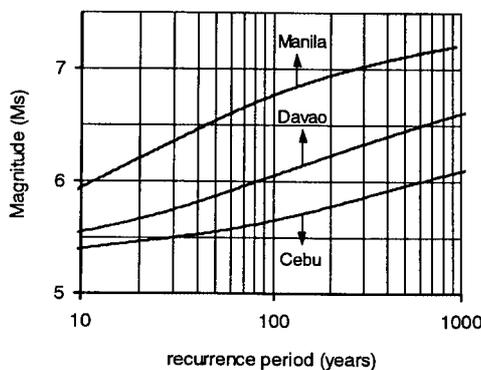
a) Hazard-consistent magnitude curve b) Hazard-consistent distance curve
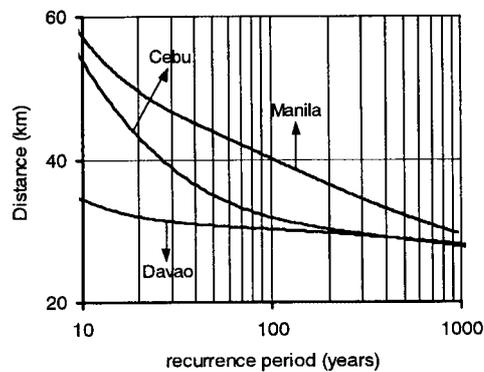
Fig. 15 Hazard-consistent magnitude and hypo-central distance curves for the three major Philippines cities

SIMULATED GROUND MOTION TIME HISTORIES FOR MANILA   RESPONSE SPECTRA

MAGNITUDE = 6.8 Ms
HYPOCENTRAL DIST. = 40.1 km

ACCELERATION

VELOCITY
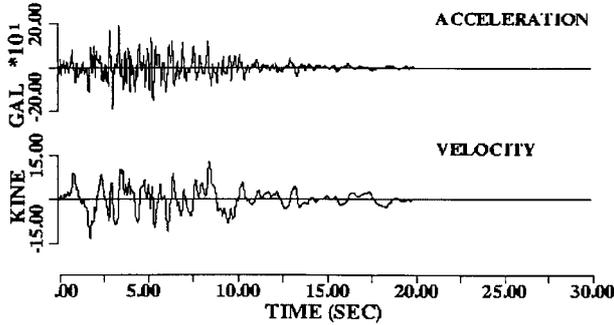
Amax = -190.8 gal   Vmax = -13.4 kine Dmax = 3.4 cm
A^{e}max = 93.0 gal   MMI = VII

DAMPING = 0.02, 0.05, 0.10, 0.20
ACCELERATION (GAL)
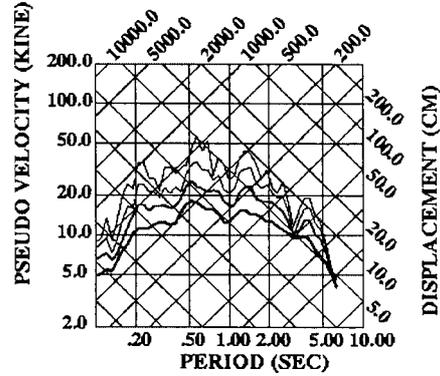
SIMULATED GROUND MOTION TIME HISTORIES FOR CEBU

MAGNITUDE = 5.7 Ms
HYPOCENTRAL DIST. = 32.0 km

ACCELERATION

VELOCITY
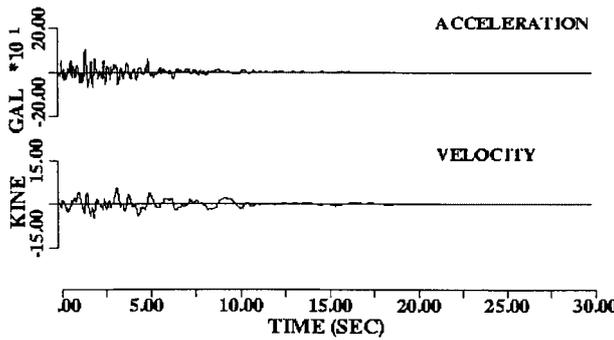
Amax = 98.4 gal   Vmax = 5.6 kine   Dmax = -.8 cm
A^{e}max = 38.0 gal   MMI = VI

DAMPING = 0.02, 0.05, 0.10, 0.20
ACCELERATION (GAL)
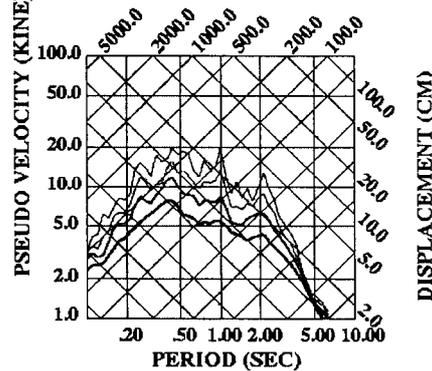
SIMULATED GROUND MOTION TIME HISTORIES FOR DAVAO

MAGNITUDE = 6.0 Ms
HYPOCENTRAL DIST. = 30.3 km

ACCELERATION

VELOCITY
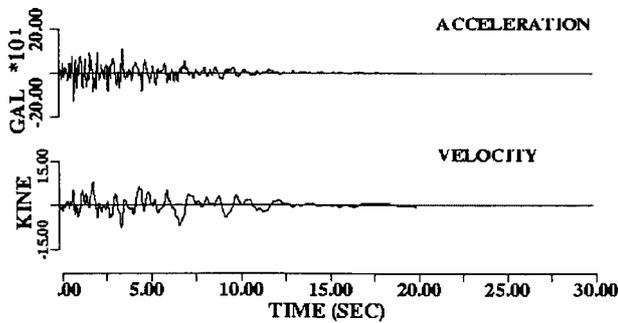
Amax = -125.9 gal   Vmax = 7.7 kine   Dmax = -1.7 cm
A^{e}max = 56.0 gal   MMI = VI

DAMPING = 0.02, 0.05, 0.10, 0.20
ACCELERATION (GAL)
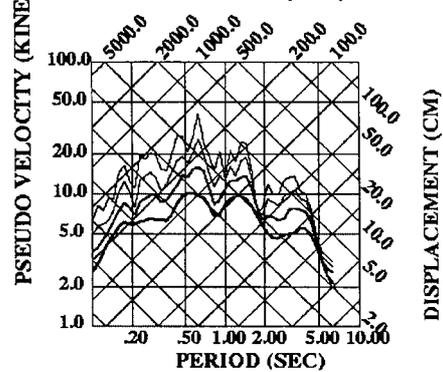
Fig. 16   Simulated rock surface strong motion for a 100-year-recurrence earthquake event.

SIMULATED GROUND MOTION TIME HISTORIES FOR MANILA

MAGNITUDE = 7.1 Ms
HYPOCENTRAL DIST. = 32.2 km
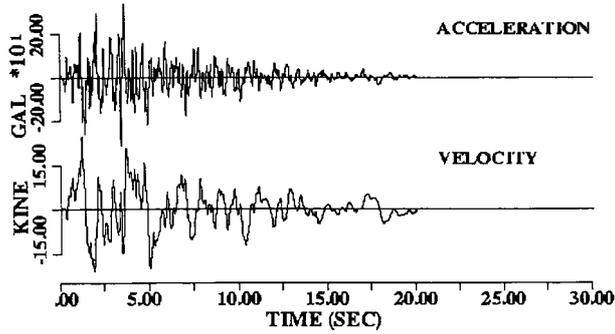
RESPONSE SPECTRA

Amax = 343.5 gal   Vmax = 24.6 kine   Dmax = 7.4 cm
A^e max = 178.0 gal   MMI = VIII
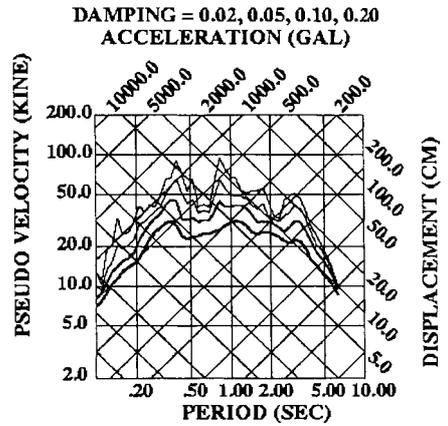
SIMULATED GROUND MOTION TIME HISTORIES FOR CEBU

MAGNITUDE = 5.9 Ms
HYPOCENTRAL DIST. = 28.8 km
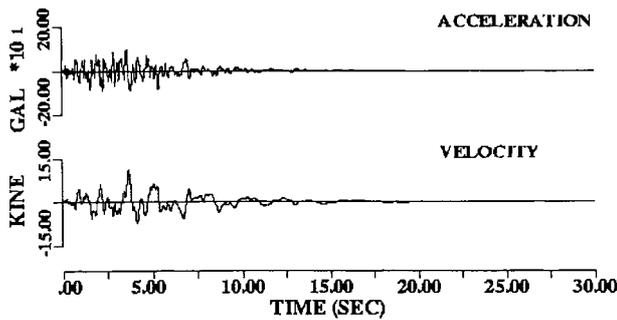
Amax = 96.2 gal   Vmax = 11.3 kine   Dmax = -1.7 cm
A^e max = 60.0 gal   MMI = VI
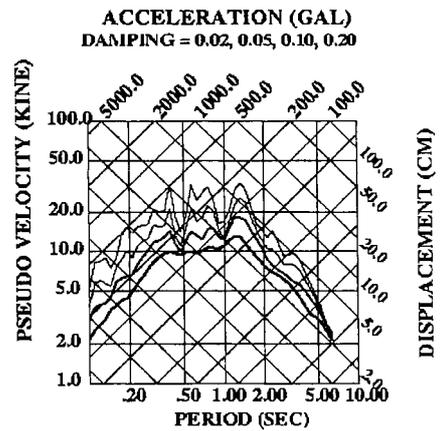
SIMULATED GROUND MOTION TIME HISTORIES FOR DAVAO

MAGNITUDE = 6.5 Ms
HYPOCENTRAL DIST. = 28.9 km
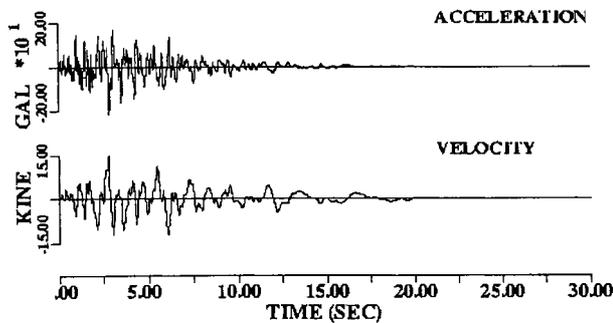
Amax = -212.3 gal   Vmax = 14.7 kine   Dmax = 2.3 cm
A^e max = 98.0 gal   MMI = VII
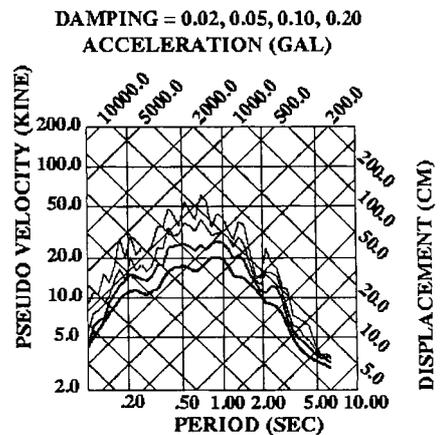
Fig. 17   Simulated rock surface strong motion for a 475-year-recurrence earthquake event.

Philippine cities for recurrence periods of 100 and 475 years were determined (Table 6).

Results indicate that Manila has a much higher hazard-consistent magnitude than Cebu or Davao. For the recurrence period of T=100 years, the expected magnitude for Manila is M_s =6.8 (M_J=6.8), whereas for Cebu and Davao respectively it is M_s=5.7 (M_J=5.9) and M_s=6.0 (M_J=6.2). For the recurrence period of T=475 years, the expected magnitude for Manila is M_s=7.1 (M_J=7.0), whereas for Cebu and Davao respectively it is M_s=5.9 (M_J=6.1) and M_s=6.5 (M_J=6.5). These hazard-consistent magnitudes depend on the properties of the zones in which the cities are located. Manila has a much bigger hazard-consistent magnitude than Cebu or Davao because the **b**-value in zone 10 is much smaller than the values in zones 18 and 23. The **b**-value is not the only factor, however. If we look at zones 18 and 23, the former has a slightly lower **b**-value, but Cebu has a lower expected magnitude than Davao. This is because the maximum magnitude at zone 18 is only 6.7, whereas in zone 23, it is 7.4. This is why Davao has a higher expected magnitude than Cebu.

For the recurrence period of T=100 years, the expected hypocentral distance for Manila is 40.1 kilometers, whereas for Cebu it is 32 kilometers and for Davao 30.3 kilometers. For rare events with the recurrence period of T=475 years, the expected hypo-central distance for Manila is 32.2 kilometers, for Cebu 28.8 kilometers and for Davao 28.9 kilometers. The importance of solving the hazard-consistent magnitude and distance is shown by the use of these parameters to simulate strong motion time histories. Ground motion time histories were simulated by inserting these parameters in the strong motion prediction model described in section 4.1.

On the basis of the hazard-consistent magnitude and hypocentral distance, the strong motions corresponding to 100-year- and 475-year-recurrence periods were simulated for Manila, Cebu, and Davao. Simulated strong motions for occasional events or the 100-year recurrences for Manila, Cebu and Davao are shown in Fig. 16. The simulated strong motions for Manila, Cebu and Davao gave respective A_{max} values of 190.8, 98.4, and 125.9 gal; V_{max} values of 13.4, 5.6, and 7.7 cm/sec; and D_{max} values of 3.4, 0.8, and 1.7 cm. Response spectra for different percentages of damping are shown. The ground motion intensity in Manila, based on the Modified Mercalli Intensity scale, is VII, whereas for Cebu it is VI and for Davao VI in MMI. For rare events corresponding to a recurrence time of 475 years, strong motions for each city also were simulated(Fig. 17): for Manila A_{max} of 343.5 gal, Cebu 96.2 gal, and Davao 212.3 gal and respective V_{max} values of 24.6, 11.3, and 14.7 cm/sec; and D_{max} values of 7.4, 1.7, and 2.3 cm. The ground motion intensity for Manila is VIII MMI, and for Cebu and Davao, respectively VI and VII in MMI. The simulated strong motions are rock surface ground motions, soil conditions not being considered. Ground motion amplification for different soil types is beyond the scope of this study.

5.   CONCLUSIONS

The major conclusions obtained are

1.   In the systematic seismic source zoning done for the Philippines, based on the occurrence rates of historical earthquakes, totally 27 seismic source zones were designated for seismic hazard analysis. No seismic source zones were assigned in the western portion of the country which is known to be aseismic.

2.   In the seismic hazard analysis done for the Philippines, based on historical earthquakes and active faults, 123,727 points were analyzed equivalent to a grid size of 1.4 kilometers. Results showed that the eastern portion of the country is under much greater seismic hazard due to movement of the Philippine Trench. Seismic hazard analyses also were made for the three major cities Manila, Cebu, and Davao, and the hazard-consistent earthquake magnitude and hypocentral distance for each city calculated.

3.   Strong motion time histories based on the hazard-consistent magnitudes and hypocentral distances corresponding to 100- and 475-year recurrence periods for the three major Philippine cities were simulated. Of these cities, the capital, Manila, has the highest seismic hazard followed in order by Davao and Cebu. The methodology for simulating strong ground motion based on seismic hazards can be used for the earthquake-resistant design of structures. Work on amplification corrections for the various geological conditions in the Philippines is in progress.

REFERENCES

Acharya, H. K., J. F. Ferguson, and V. Isaac, 1979. Microearthquake surveys in the central and northern Philippines, *Bulletin of the Seismological Society of America*, 69: 6. 1889-1902.

Acharya, H. K. , 1980a. Seismic and tsunamic risk in the Philippines, *Proc. 7th World Conf. On Earthquake Engineering* 1: 391-394.

Acharya, H. K. , 1980b. Regional variations in the rupture length – magnitude relationships, *Proc. 7th World Conf. On Earthquake Engineering*, 1: 193-196.

Applied Technology Council (ATC-13), 1985. Earthquake damage evaluation data for California, *Appendix B: Seismological Intensity Scales*, 337.

Barrier, E., P. Huchon, and M. Aurelio, 1991. Philippine Fault: A key for Philippine kinematics, *Geology*, 19: 32-35.

Chiaruttini, C. and L. Siro, 1981. The correlation of peak ground horizontal acceleration with magnitude, distance, and seismic intensity for Friuli and Ancona, Italy and Alpide belt, *Bulletin of the Seismological Society of America*, 71: 6. 1993-2009.

Fukushima, Y. and T. Tanaka, 1991. A new attenuation relation for peak horizontal acceleration of strong earthquake motionsin Japan, *Bulletin of the Seismological Society of America*, 80, 757-783.

Hayashi, Y. and K. Abe, 1984. A method of MS determination from JMA data, *Journal of the Seismological Society (JSCE)*, 37: 429-439 (in Japanese).

Katayama, T., 1982. An engineering prediction model of acceleration response spectra and its application to seismic hazard mapping, *Earthquake eng. struct. dyn.*, 10: 149-163.

Kameda, H., 1975. Evolutionary spectra of seismogram by multifiltere, *Journal of engineering mechanics, ASCE*, 101: 787-801.

Kameda, H. and N. Nojima, 1988. Simulation of risk consistent earthquake motion, *Earthquake eng. struct. dyn*, 16: 1007-1019.

Knittel, U., M. J. Defant, and I. Raczek, 1988. Recent enrichment in the source region of arc magmas from Luzon Island, Philippines: Sr and

Nd isotopic eveidence, *Geology*, 16: 73-76.

Lanuza, L. G., 1999. List of Philippine earthquakes as compiled by the Philippine Institute of Volcanology and Seismology (PHIVOLCS), (*personal correspondence by email*).

Molas, G. L. and F. Yamazaki, 1994. Seismic macrozonation of the Philippines based on seismic hazard analysis, *Structural Eng. /Earthquake Eng. (JSCE), II:I;* 33s-43s .

Mualchin, L., 1996. A technical report to accompany the CALTRANS California seismic hazard map (Based on maximum credible earthquakes), *Open file Report, California Department of Transportation Engineering Service Center*, http://www. dot. ca. gov/hq/esc/ earthquake_engineering/Seismology/MapReport. PDF.

Pacheco, B. M., 2000. Development of seismic loading provisions in the National Structural Code of the Philippines, *2nd Multi-lateral Workshop on Development of Earthquake and Tsunami Disaster Mitigation Technologies and its Integration for the Asia-Pacific Region*, Kobe, Japan, March 1&2, 2000.

Rast, B. and R. Saegesser, 1980. On the systematics in defining seismic zones, *Proc. 7th World Conf. on Earthquake Engineering*, 1: 261-268.

Sajona, F. G., R. Maury, H. Bellon, J. Cotten, M. Defant, and M. Pubellier, 1993. Initiation of subduction and the generation of slab melts in western and eastern Mindanao, the Philippines, *Geology*, 21: 1007-1010.

Shimazaki, K., and T. Nakata, 1980. Time-predictable recurrence model for large earthquakes, *Geophysical Research Letters*, 7: 279-282.

Slemmons, D. B., 1978. Determination of design earthquake magnitudes for microzonation, *Proceedings of the Second International Conference on Microzonation*, 1: 119-130.

Su, S. S., 1980. Attenuation of intensity with epicentral distance in the Philippines, *Bulletin of the Seismological Society of America*, 70: 1287-1291.

Sugito, M., 1995. Frequency-dependent equivalent strain for earthquake response analysis of soft ground, *Proceedings of the IS-Tokyo, '95, The First International Conference on Earthquake Geotechnical Engineering*, Tokyo, 655-660.

Sugito, M., Y. Furumoto, and T. Sugiyama, 2000. Strong motion prediction on a rock surface by superimposed evolutionary spectra, *12th World Conference on Earthquake Engineering*, Auckland, New Zealand, January 2000.

Villaraza, C. M., 1991. *A Study on the seismic zoning of the Philippines, Proceedings. 4th International Conference on Seismic Zonation*, 3: 511-518.